Evolutionary Intelligence (2021) 14:1775–1792
https://doi.org/10.1007/s12065-020-00456-y

RESEARCH PAPER

Artificial intelligence and game theory controlled autonomous UAV swarms

Janusz Kusyk[1] · M. Umit Uyar[2] · Kelvin Ma[2] · Eltan Samoylov[2] · Ricardo Valdez[2] · Joseph Plishka[3] · Sagor E. Hoque[3] · Giorgio Bertoli[3] · Jeffrey Boksiner[3]

Received: 27 January 2020 / Revised: 8 June 2020 / Accepted: 22 June 2020 / Published online: 25 July 2020

Abstract
Autonomous unmanned aerial vehicles (UAVs) operating as a swarm can be deployed in austere environments, where cyber electromagnetic activities often require speedy and dynamic adjustments to swarm operations. Use of central controllers, UAV synchronization mechanisms or pre-planned set of actions to control a swarm in such deployments would hinder its ability to deliver expected services. We introduce artificial intelligence and game theory based flight control algorithms to be run by each autonomous UAV to determine its actions in near real-time, while relying only on local spatial, temporal and electromagnetic (EM) information. Each UAV using our flight control algorithms positions itself such that the swarm maintains mobile ad-hoc network (MANET) connectivity and uniform asset distribution over an area of interest. Typical tasks for swarms using our algorithms include detection, localization and tracking of mobile EM transmitters. We present a formal analysis showing that our algorithms can guide a swarm to maintain a connected MANET, promote a uniform network spreading, while avoiding overcrowding with other swarm members. We also prove that they maintain MANET connectivity and, at the same time, they can lead a swarm of autonomous UAVs to follow or avoid an EM transmitter. Simulation experiments in OPNET modeler verify the results of formal analysis that our algorithms are capable of providing an adequate area coverage over a mobile EM source and maintain MANET connectivity. These algorithms are good candidates for civilian and military applications that require agile responses to the changes in dynamic environments for tasks such as detection, localization and tracking mobile EM transmitters.

Keywords AI · Game theory · MANET · Autonomous UAV · Swarm · Bio-inspired computation

1 Introduction

Autonomous unmanned aerial vehicles (UAVs) operating as a swarm can be deployed in austere environments, where cyber electromagnetic activities often require speedy and dynamic adjustments to swarm operations. Use of central controllers, UAV synchronization mechanisms or pre-planned set of actions to control a swarm in such deployments would hinder its ability to deliver expected services. Rapid deployment, high scalability and responsiveness required by many civilian and military applications demand decentralized wireless networks without rigid infrastructures, which necessitates that swarm members form and maintain mobile ad-hoc networks (MANETS) to accomplish complex mission objectives. MANETS are particularly suitable to operate in austere three-dimensional tactical situations, where self-deployment of autonomous mobile nodes is critical for maintaining a dynamic network topology. Using wireless multi-hop communication, MANET nodes are capable of forming non-hierarchical topologies that change unpredictably over time. These desirable characteristics of MANETS at the same time bring new challenges for providing autonomous

✉ M. Umit Uyar
uyar@ccny.cuny.edu

[1] NYC College of Technology, City University of New York, Brooklyn, NY 11201, USA

[2] The City College of New York, City University of New York, New York, NY 10031, USA

[3] I2WD, US Army CCDC - C5ISR Center, Aberdeen Proving Ground, MD 21005, USA

flight control of UAVs operating as a swarm, including an increased level of topology control and cyber security.[1]

Bio-inspired computation techniques are excellent candidates to bring effective solutions for MANET topology control [50], routing [20], node collaboration[36] and cybersecurity mechanisms[25]. These techniques can find desired optimum or near optimum solutions to satisfy conflicting objectives in prohibitively large domains. They emulate evolutionary processes found in nature, where better adapted individuals have greater chances of survival in an environmental niche.

We have shown that autonomous UAVs can operate as a self-organized swarm demonstrating an emergent behavior needed to accomplish complex missions in severe military environments[50]. Each autonomous UAV in a swarm can make its own decisions using bio-inspired algorithms to obtain adequate solutions for multi-objective optimization problems. Despite locality of individual mobile node decisions, a swarm of UAVs can exhibit the responsiveness needed for, for example, maintaining MANET connectivity in dynamically changing environments[17]. This agility can only be achieved by fast and lightweight bio-inspired algorithms guiding each UAV's flight control decisions.

Game theory (GT) based solution techniques has become popular for solving problems with multiple and often competing goals in a wide range of fields including economics, finance and political science. GT offers excellent tools to analyze behavior of rational and selfish players in strategic situations, where outcomes depend on actions of all participants. In engineering applications, GT has been shown to be effective in computer communications especially for multi-objective optimization problems in network resource allocation, routing efficiency and intrusion detection systems. For many MANET operations (e.g., topology control of mobile nodes), GT analyzes incentives and deterrents built into mobile node actions to provide desired solutions, thus eliminating need for node coordination and synchronization[22, 26].

We introduce artificial intelligence (AI) and game theory (GT) based flight control algorithms to be run by each autonomous UAV to determine its actions in near real-time, while relying only on local spatial, temporal and electromagnetic (EM) information. Each UAV using our flight control algorithms positions itself such that the swarm maintains mobile ad-hoc network (MANET) connectivity and uniform asset distribution over an area of interest. Typical tasks for swarms using our algorithms include detection, localization and tracking of mobile EM transmitters.

We present a formal analysis showing that our algorithms can guide a swarm to maintain a connected MANET, promote a uniform network spreading, while avoiding overcrowding with other swarm members. We also prove that, while maintaining MANET connectivity, they can simultaneously lead a swarm of autonomous UAVs to follow or avoid an EM transmitter. Simulation experiments in OPNET Modeler verify the results of formal analysis that our algorithms are capable of providing an adequate area coverage over a mobile EM source and keep the MANET connected.

The rest of this paper is organized as follows. Section 2 highlights recent research in flight control and bio-inspired algorithms for governing MANET topology. Section 3 introduces our bio-inspired and GT based flight control algorithms for UAV swarms. We introduce a formal analysis our algorithms with respect to their capability of uniform spreading spreading and tracking a EM source are presented in Sect. 4. Results of OPNET simulation experiments to evaluate their performance for different swarm configurations are presented in Sect. 5. Consideration of multiple mobile EM sources are discussed in Sect. 6. Finally, concluding remarks and future research directions are in Sect. 7.

2 Related work

In this section, we present a summary of recent research results in UAVs operating as swarms, bio-inspired AI computation techniques designed to govern such systems and applications of GT to MANETs. As we highlight the scope of these studies we point out their potential to be applicable to dynamic and austere theaters in civilian and military settings and their possible limitations as they relate to the flight control of swarms of autonomous UAVs.

2.1 Swarms of UAVs

Several recent studies proposed the use of global control mechanisms over swarms of UAVs in order to control their actions as they accomplish a given task. For example, centralized mission planners to distribute tasks to UAVs are suggested in[35], whereas a global coordination among swarm members is discussed in[10]. A pre-planned 3D distribution of multiple UAVs is performed to optimize power used by each aircraft in[2]. Similar approaches to control UAVs include partially autonomous UAVs that need periodic interactions with a centralized (often ground-based) controller to eliminate long-distance communication links in[5] and costly image processing and coordination procedures running in UAVs designed for tasks such as topology formation and obstacle avoidance[6]. In[48], UAVs require coordination procedures and target state sharing in their ant colony based task allocation mechanism.

[1] Throughout the paper the term MANET refers to the mobile ad hoc network established among autonomous UAVs in a swarm.

Tactical networks can be arranged as hybrid aerial and terrestrial communication systems to facilitate public safety connectivity if communication infrastructure becomes damaged[4, 28]. Some semi-autonomous swarms are designed with a pre-determined set of UAV actions to operate in known territories[1], while other flight control algorithms typically rely on a remote authority controlling a single stand-alone UAV to improve transmission rates and coverage of a target area[30]. Distributed control algorithms for UAV swarms tasked with terrain mapping is proposed in[39], while[14] investigates wind gust resiliency of small UAVs participating in surveillance missions using swarm clustering methods. An adaptable autonomy of UAV swarms, where commands are sent to a swarm via a ground station for path-planning with collision avoidance capabilities through simulations are presented in[42].

These proposed methods may not be adequate for controlling a swarm of autonomous UAVs operating in dynamic environments since unpredictably and speedily changing conditions will nullify pre-planned procedures, whereas attempts of centralized control will ultimately be too slow to respond the task requirements.

2.2 Bio-inspired computation for swarms and UAVs

Within the realm of artificial intelligence (AI) based computation techniques, bio-inspired computation techniques (BCTs) mimic evolutionary processes promoting well adopted group of organisms to reproduce and prevail as a population in a given environmental niche. Effective design and implementation of BCT algorithms can provide suitable outcomes for problems with conflicting objectives, while involving light computational loads. BCTs gained popularity in networking due to their ease of implementation and effectiveness to solve multi-objective and often intractable optimization problems, including MANET topology control[50], routing[13, 20], node collaboration[36] and cybersecurity[25].

Coordinating a swarm of UAVs to provide continuous coverage of an area of interest, identified as an intractable problem[38], can be effectively handled by evolutionary bio-inspired techniques. An adequate deployment of a swarm of UAVs can be obtained by applying particle swarm optimization techniques[7] while path planning for multi-objective missions can be achieved using genetic algorithms[33, 40] and artificial ant colony optimization[49] methods. A leader–follower coalition formation in swarms with large number of UAVs, each with limited communication and energy capabilities, was proposed in[29] by employing quantum genetic algorithms.

In our previous research[50], using bio-inspired algorithms to solve multi-objective optimization problems, autonomous vehicles are shown to operate as a self-organizing swarm in austere environments. Each individual in a swarm makes its own decisions using BCT algorithms to solve a given problem, yet, despite locality of individual mobile node decisions, the swarm can maintain the pace needed for preserving MANET connectivity[17]. We also show that our BCT algorithms are fast and lightweight in guiding mobile nodes and they can provide adequate fault tolerance and resilience under rapidly changing conditions[34].

2.3 Game theory applications for swarms and UAVs

Game theory (GT) is a framework for analyzing behavior of rational competitors in strategic situations, where outcomes depend on actions of all players. GT is a specific area of applied mathematics whose scope encompasses a broad set of analytical techniques for real-life problems in economics, business, planning, engineering, science and others. Popular applications of GT in telecommunication networks attempt to design efficient routing protocols with enhanced security and improved spectrum sharing[8, 9, 19]. In our previous research we demonstrated that GT can provide fault-tolerant topology control for autonomous nodes in MANETS that gracefully recover from adversarial actions in 2- and 3-dimensional tactical scenarios in theatres with and without obstacles obstructing the movements of mobile nodes[18, 21, 26].

Significance of GT for UAV control has been demonstrated in several recent research results, including detection of attacks on UAVs that augment ground sensor and vehicular networks[37], task allocation in a swarm of drones visiting multiple locations[16] and providing decentralized coalition formation of UAVs for search and neutralization of targets[3]. Flight control systems to coordinate UAVs based on *cooperative games* are reported in[41].

A game is proposed in[44] for a group of autonomous UAVs, where each UAV is tasked with collecting information from an area of interest. In this setting, a mission to maximize the amount information of collected by UAVs is formulated by dividing the region of interest into discrete cells, each having an associated information value. Each selfish UAV (i.e., player) makes the best decision for itself by selecting a path among available choices (i.e., strategies) that it will fly. Game payoffs are determined using *information fusion*[27] for aggregating information from multiple UAVs operating on multiple locations. Efficiency of a mission is the ratio of an optimal output to a pure strategy Nash equilibrium[31] for the corresponding game.

Stackelberg games[47] can be used to obtain flight routes for UAVs operating in areas with malicious parties carrying out GPS spoofing attacks aimed to divert UAVs from their original flight paths[12]. In a Stackelberg game between a UAV operator acting as the game leader and a GPS spoofer, the

leader chooses a group of UAVs to protect, after which the spoofer determines its actions after observing the decision of the leader. Strategies in this game reflect abilities of each UAV to estimate its location using positions of its nearby UAVs and, hence, allowing it to reach a destination despite ongoing GPS spoofing attacks.

2.4 Our previous research

The study presented in this paper builds on the preliminary results reported in[23, 24]. We introduced initial versions of our near real-time flight control algorithms that combine GT and bio-inspired computation techniques to effectively guide autonomous UAVs in[23]. In[24], we studied the use 3D Voronoi tessellations and linear interpolation techniques for mapping EM landscape using local neighbor information.

In this paper, (i) we combine and extend evolutionary algorithms and non-cooperative game models to automatically handle different modes of operations such as spreading and tracking, (ii) we build our new evolutionary algorithms by introducing adjustment parameters that are essential to make flight control dynamically adaptable to unpredictable changes in EM landscape, (iii) we introduced a new non-cooperative game that factors in the information from neighbors of neighbors in predicting the outcomes of neighbor movements to marginalize network partitioning, (iv) we formally analyzed the properties of evolutionary algorithms working together with non-cooperative games for flight control of swarms of autonomous UAVs operating in spreading and tracking modes, and (v) we introduced new performance metrics and conducted extensive simulation experiments to validate the formal analysis results.

3 Our UAV control algorithms

A swarm of autonomous UAVs guided by our flight control algorithms aims to respond to a mobile EM source by either avoiding it or shadowing EM transimitter movements while upholding network connectivity. In a typical operation, a swarm may be deployed to zero-in on an EM source while providing ongoing uninterrupted communication or position, navigation, and timing services to dispersed ground and low-altitude entities. This task is especially challenging when the swarm is expected to respond to unpredictable changes in austere conditions.

In our system, a bio-inspired evolutionary algorithm, called evolutionary flight control (EFC), will be run by each autonomous UAV. There are several choices to realize EFC algorithms, including genetic algorithms, particle swarm optimization, and differential evolution[45]. For the sake of simplicity, we used a genetic algorithm to implement the EFC in the simulation experiments reported in this paper.

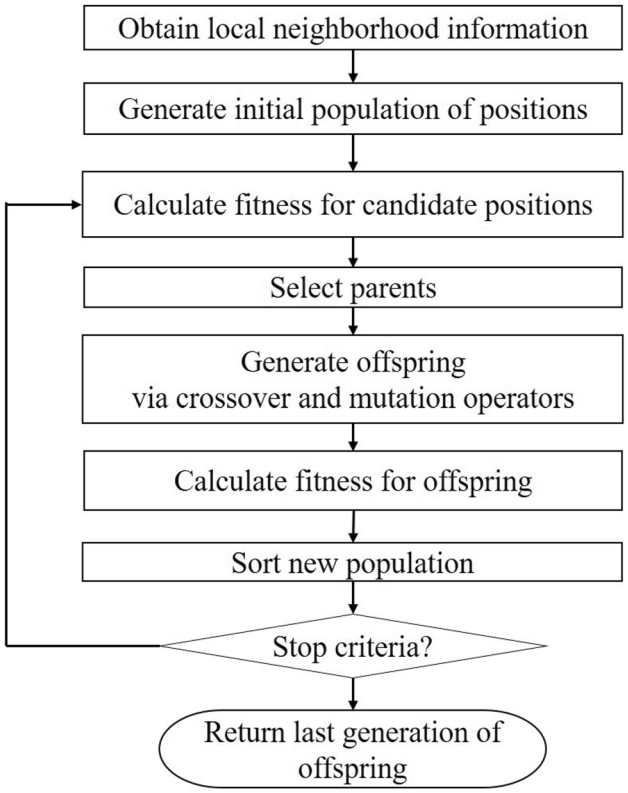

Fig. 1 Flow chart for implementing EFC by a genetic algorithm

With EFC, a UAV finds a set of candidates for improved next locations in the 3D space around the UAV. These candidate positions are then used as strategies in a realistic self-enforcing non-cooperative game[15] set up among a UAV and its near neighbors, where game payoffs reflect the actions of players. In our game, called non-cooperative decision game (NCDG), a selfish UAV selects a next position by anticipating the next actions of its neighbors to maximize its payoff. UAVs guided by our EFC and NCDG promote emergent swarm intelligence and self-organization needed for efficient response to ever-changing conditions. Our goal is to form a swarm of autonomous UAVs which can track by following or avoiding a mobile EM target, while keeping a high percentage ground area coverage and MANET connectivity throughout a mission. EFC and NCDG are designed to only require information from near neighbors of a UAV to determine its actions in near real-time.

3.1 Bio-inspired evolutionary algorithm

A flow chart describing the operation of our EFC, which will be run in each UAV for flight control, is given in Fig. 1. In our implementation of EFC, a chromosome represents a candidate next position for the UAV to move. EFC starts with generating a population of individuals (i.e., candidate positions).

3.1.1 Fitness function

The fitness $\mathcal{F}_i$ of a candidate location for UAV n_i with $\mathcal{N}_i(t)$ neighbors at time t is defined as

$$\mathcal{F}_i = \begin{cases} \gamma(t,p_i)\sum_{j=1}^{\mathcal{N}_i(t)} D_{ij} & \text{if } |\mathcal{N}_i(t)| \geq 1 \\ \mathcal{M}_c & \text{otherwise} \end{cases} \quad (1)$$

where $\mathcal{M}_c$ is the maximum penalty applied to a location that would result in n_i being disconnected from its neighbors and D_{ij} is the virtual force applied to n_i by its neighbor n_j as will be explained in detail in Eq. (3). For all practical applications, $\mathcal{M}_c$ should have a greater value than any feasible $\mathcal{F}_i$; for example, if the number of near neighbors for n_i at time t is $|\mathcal{N}_i(t)| \geq 1$, it is possible to set $\mathcal{M}_c > (R_c \times |\mathfrak{N}|)$, where $|\mathfrak{N}|$ is the total number of deployed UAVs and R_c is the communication range of n_i. Smaller fitness values for $\mathcal{F}_i$ in Eq. (1) indicate preferable positions for a UAV to move. Note that because the EM transmitter and UAV swarm are mobile, system parameters such as γ and $\mathcal{N}_i$ include time t in their definitions.

The weight $\gamma(t,p_i) \in (0,1]$, computed at time t for a local position p_i, incentivizes locations with stronger (or weaker) received signal strength and, hence, promotes a swarm emergence needed for a preferred course of action (e.g., following or avoiding) a mobile EM source. Basic off-the-shelf hardware components included in payload would enable a UAV to measure the signal strength on a frequency used by an EM transmitter at time t and a local position p_i as $\text{RSS}(t,p_i)$. A swarm can use this information to direct its members as needed to track by following or avoiding a mobile EM transmitter in a given theatre.

In this implementation, each UAV periodically broadcasts its location and RSS information to its near neighbors within R_c range. Using location and signal strength information from its near neighbors, it is possible for a UAV to compute characteristics of its EM landscape. Therefore, fitness $\mathcal{F}_i$ given in Eq. (1) selects preferable candidates with respect to both topology and EM landscape criteria.

In our flight control algorithms, we define $\gamma(t,p)$ as

$$\gamma(t,p_i) = (1+\epsilon) - \left[\frac{\alpha\,(\text{RSS}(t+1,p_i) - \text{RSS}(t,p_{\mathcal{N}_i}^{min}))}{\text{RSS}(t,p_{\mathcal{N}_i}^{max}) - \text{RSS}(t,p_{\mathcal{N}_i}^{min}) + \epsilon} \right] \quad (2)$$

where $\text{RSS}(t,p_{\mathcal{N}_i}^{max})$ and $\text{RSS}(t,p_{\mathcal{N}_i}^{min})$ are the maximum and minimum RSS measurements recorded until time t in near neighbors of n_i (i.e., $\mathcal{N}_i$), respectively, and a small ϵ prevents denominator from being zero. $\text{RSS}(t+1,p_i)$ is the predicted signal strength at the candidate location p_i. The value for $\text{RSS}(t+1,p_i)$ can be calculated by means of several different methods such as Voronoi tessellations and linear interpolation as introduced in our earlier work[24]. Parameter $\alpha \in (0,1]$ controls how aggressively UAV n_i will track by following or avoiding a mobile EM source. When $\alpha \approx 1$, candidate locations satisfying $\text{RSS}(t+1,p_i) \approx \text{RSS}(t,p_{\mathcal{N}_i}^{max})$ would significantly scale down the fitness value $\mathcal{F}_i$ as computed by Eq. (1) to let a swarm follow or avoid a mobile EM source. On the other hand, when α is chosen close to zero, candidate positions with high $\text{RSS}(t+1,p_i)$ will have lesser impact on $\mathcal{F}_i$ and, hence, swarm spreading is prioritized over the influence of the EM source.

Selection of α can be dynamically determined during a swarm operation. For example, if it is noticed by received signal strength that an EM transmitter is moving away (i.e., a few consecutive RSS readings from a UAV indicate that there is a decrease in EM values such as $\text{RSS}(t-1,p_i) > \text{RSS}(t,p_i)$), α can be increased to motivate the UAVs to consider EM impact in the fitness. Similarly, if EM landscape is relatively static over a period of time (i.e., $\text{RSS}(t-1,p_i) \approx \text{RSS}(t,p_i)$), α can be increased emphasize the uniform distribution rather than EM source.

In Eq. (1), D_{ij} denotes the virtual force applied to n_i by its neighbor n_j as a function of Euclidean distance between them $d(n_i,n_j)$. The virtual force D_{ij} between n_i and n_j is

$$D_{ij} = \begin{cases} R_c - d(n_i,n_j) & \text{if } 0 < d(n_i,n_j) \leq d_{th} \\ \eta & \text{if } d_{th} < d(n_i,n_j) \leq \mathcal{R}_m(t) \end{cases} \quad (3)$$

where η is a small number, d_{th} defines a threshold value for the best node separation with a sufficiently small η, and $\mathcal{R}_m(t)$ is the movement range for n_i as defined below. The threshold value d_{th} and η eliminate unnecessary loitering (i.e., in-air jittering) of UAVs that are already separated from each each other by searching for marginally better positions and, hence, reduce a chance for a fast moving n_i of accidentally disconnecting from n_j when $d(n_i,n_j) \approx R_c$. In real implementations, d_{th} should be selected as a small fraction of R_c.

3.1.2 Node movement and speed

When running an implementation of EFC, a UAV calculates a set of next locations within a sphere of radius $\mathcal{R}_m(t)$ units away from itself such that

$$\mathcal{R}_m(t) \leq \frac{R_c - d(n_i,n_j^c)}{\theta(t)} \quad \text{with } \theta(t) \in (2,v] \quad (4)$$

where $n_j^c \in \mathcal{N}_i(t)$ is the closest neighbor of n_i (i.e., $\forall n_k \in \mathcal{N}_i(t),\ d(n_i,n_j^c) \leq d(n_i,n_k)$) and $\theta(t)$ is an adjustment parameter for controlling range of movement at time t. Parameter $\theta(t)$ determines the space of candidate locations for a UAV to move at time $(t+1)$. Selection of $\theta(t)$ value depends on the phase of a swarm deployment. In the early stages of a deployment, where many UAVs are close to each

other, $\theta(t)$ should be selected to be closer to its lower limit of 2, whereas $\theta(t) \approx v$ (e.g., $v = 3, 4, \ldots$) is preferred for later steps, as the set of next location candidates need to be more precise.

This mechanism of time-varying selection of movement space implies that UAVs initially move faster and consider larger spaces around them for making movement decisions. As UAVs get closer to be in a uniform distribution, smaller steps must be taken by adjusting $\theta(t)$ properly so that network partitioning is avoided.

3.1.3 EFC operation

After calculation of fitness, individuals in a population are sorted based on their fitness values. Using a selection mechanism (see Fig. 1), parents are chosen giving preferences to better individuals (i.e., an *elitist* selection mechanism). Then, by means of a single- or multiple-point *cross-over* operator, offspring is generated from preferred parents. In EFC implementation a low-probability *mutation* operator is used to avoid candidate positions that represent local minima in their vicinity. EFC calculates the fitness of offspring and includes them into the population such that only the better performing individuals are kept for the next generation.

3.1.4 Termination conditions

The algorithm stops after running a pre-determined number of generations or when no fitness improvement is detected for a few generations. Individuals from the last generation of offspring, called Λ^L, are evaluated by our NCDG to select a next position that would benefit the UAV itself as well as its near neighbors, as explained in Sect. 3.2. With its linear complexity, our implementation of EFC as outlined in Fig. 1 is computationally inexpensive.

3.2 Game theory algorithms

In our flight control algorithms, EFC provides a computationally lightweight method for finding a set of promising locations in dynamic environments, whereas NCDG promotes adequate next positions that benefit both the moving UAV and the swarm connectivity and spread. Figure 2 outlines operations of our game set up by a UAV against its neighbors when determining its next location to move.

An autonomous UAV n_i determines its next position by setting the game $\Gamma_i(t) = \langle P, S, U \rangle$ with its near neighbors at time t. In $\Gamma_i(t)$, we define a set of players $P = \{n_i \cup \mathcal{N}_i(t)\}$, a space of strategy profiles $S = \times_{n_k \in P} S_k$, where strategy space for player n_k is $S_k = \{\Lambda^L \cup p_k\}$ with Λ^L representing the candidates obtained at the last generation of EFG and p_k denoting the location of n_k at time t ($\times$ symbolizes the Cartesian product operator). A tuple U of payoffs, often referred to as

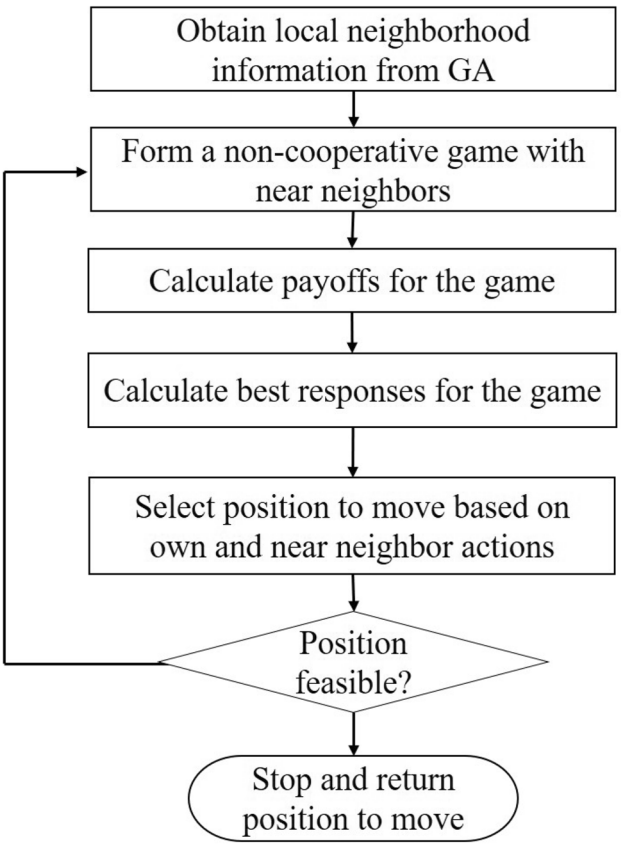

Fig. 2 High level sketch for a game to be run by a UAV

utilities, reflects preferences for all players over the game outcomes. For each $n_k \in P$, payoff is its anticipated fitness $\mathcal{F}_k$ in Eq. (1) when *strategy profile* called $\boldsymbol{s} \in S$, with the next locations of each UAV in P, is realized.

A *payoff function* for player n_i, when strategy profile $\boldsymbol{s}$ is realized, is defined as $\mathcal{U}_i(\boldsymbol{s})$. It is a von Nuemann–Morganstern function, which reflects preferences of n_i over $\forall \boldsymbol{s} \in S$ [46]. A rational selfish player always intends to obtain the best payoff for itself. A strategy $s_i^* \in S_i$ for player n_i is called a *preferred strategy* against the strategies of its near neighbors $\mathcal{N}_i(t)$ at time t. A *deleted strategy profile* $\boldsymbol{s}_{-i}$ is a tuple reflecting strategies of near neighbors $\mathcal{N}_i(t)$ (i.e., $\boldsymbol{s}_{-i} \in \times_{n_j \in \mathcal{N}_i(t)} S_j$), hence $\boldsymbol{s} = (s_i, \boldsymbol{s}_{-i})$. In other words, strategy profile $\boldsymbol{s}$ is a combination of strategy of n_i and the strategies of its neighbors. In this case, a preferred strategy s_i^* for player n_i is defined as

$$(\forall s_i \in S_i)\ \mathcal{U}_i(s_i^*, \boldsymbol{s}_{-i}) \geq \mathcal{U}_i(s_i, \boldsymbol{s}_{-i}) \tag{5}$$

where the utility function $\mathcal{U}_i$ computes payoff for n_i moving to the location indicated by strategy s_i when its neighbors move to positions represented by a tuple of probable future locations for all UAVs in $\mathcal{N}_i(t)$. Player n_i computes the *best*

response $\mathcal{R}_i(t)$ to possible actions of its rational neighbors $\mathcal{N}_i(t)$ at time t as

$$\mathcal{R}_i(t) = \arg\min_{s_i \in S_i} \mathcal{U}_i(s_i, \boldsymbol{s}_{-i}) \tag{6}$$

for all $\boldsymbol{s}_{-i} \in \times_{n_j \in \mathcal{N}_i(t)} S_j$. For each deleted strategy profile s_{-i}, player n_i evaluates Eq. (5) to find the best strategy for itself. By using Eq. (6), selfish player n_i selects its best next location by avoiding crowding locations that could be chosen by neighboring swarm members. Using Eq. (6) prevents nodes from movements that could result in a disconnected MANET topology. It is possible that the best response of n_i can designate more than one best choice to move, where $\mathcal{R}_i(t)$ is a set of best n_i responses to possible movements of its near neighbors at time t. In such cases, n_i selects its next position based on a pre-determined criteria (e.g., selecting a position that minimizes $\sum_{n_j \in P} \mathcal{F}_j$).

3.3 Response to mobile EM transmitter

Our approach combines game theory and evolutionary computation algorithms to obtain a computationally lightweight flight control for each autonomous UAV to determine its movements in near-real time. As an EM transmitter moves, EM signal landscape that it creates changes, which then triggers UAVs to move with respect to the levels of the received EM signal strength by either following or avoiding the EM source.

The goal for each UAV is, using only local information, to react to a moving target without a priori knowledge on a target trajectory while maintaining connectivity to its neighbors. At time t, UAV n_i broadcasts its position p_i and $\text{RSS}(t, p_i)$ measurements to its neighbors at most R_c distance away. UAV n_i obtains its local 3D EM propagation heatmap by applying Voronoi tessellations[11] to the known measurement points in its locality collected by its near neighbors $\text{RSS}(t, p_j)$, $\forall j \in \mathcal{N}_i(t)$. For any point p_j reflecting the location of a neighbor $n_j \in \mathcal{N}_i(t)$ at time t, Voronoi tessellation outlines a Voronoi region V_j such that all locations closer to p_j than to any other p_k from the respective $n_k \in \{\mathcal{N}_i(t) \cup n_i\}/\{n_j\}$ are parts of V_j. We define a Voronoi region for a p_j of $n_j \in \{n_i \cup \mathcal{N}_i(t)\}$ as

$$V_j = \{\omega \in \Omega : d(p_j, \omega) < d(p_k, \omega), \forall_{p_k \in \{\mathcal{N}_i(t) \cup n_i\}/\{n_j\}}\} \tag{7}$$

where Ω represents the set of all points within R_c distance from n_i and $d(p_j, \omega)$ stands for the distance between p_j (x_j, y_j, z_j) and a point $(x_\omega, y_\omega, z_\omega)$ in Ω.

EM heatmap of the area around UAV n_i are shown in Fig. 3, where n_i is located at the center, the locations of its neighbors are represented as green dots and an EM radio emitter is marked as a target on the ground. The intensity of $\text{RSS}(t, p_j)$ (measured in dBW) for each cell are shown by the colored bar placed at the right hand side of Fig. 3.

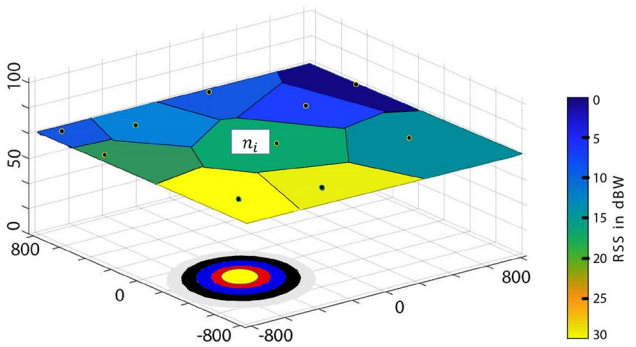

Fig. 3 EM heatmap obtained with Voronoi tessellations from $\text{RSS}(t, p_k)$ measurements at points $\forall n_k \in P$ surrounding a UAV n_i at time t

For simplicity, only a single cross-section of the 3D EM landscape is included in Fig. 3.

A sample Voronoi tessellation, which was obtained using Eq. (7), is shown in Fig. 3, where the black dot within each cell corresponds to the location of a neighbor UAV. Our flight control algorithms incorporate the anticipated $\text{RSS}(t, p_j)$ value of a candidate position p_j to guide the UAV in its movement decisions.

During swarm operation, at time t, UAV n_i computes a Voronoi-based EM heatmap of its neighborhood using Eq. (7). Based on the minimum and maximum signal strength values, $\text{RSS}^{min}(t, p_i)$ and $\text{RSS}^{max}(t, p_i)$, respectively, and the RSS values from candidate locations $\text{RSS}(t+1, p_i)$, it calculates $\gamma(t, p_i)$ as defined in Eq. (2). Using $\gamma(t, p_i)$ as the weight function, fitness $\mathcal{F}_i$ is then calculated using Eq. (1) that directs the swarm movements as response to a mobile EM transmitter.

4 Spreading and tracking analysis

In this section we introduce a formal analysis our algorithms to show that topology of UAVs converge to a uniform distribution while keeping the network connected. We also prove that the swarm is capable of tracking a mobile EM target, either by following or avoiding it, while keeping connected to its MANET.

Let us first introduce several definitions as follows.

Definition 1 Two UAVs n_i and n_j operating in a swarm are called near neighbors if $d(n_i, n_j) \leq R_c$ units, where R_c is the communication range for these UAVs.

Definition 2 A communication path between two UAVs n_i and n_j is a path between n_i and n_j with one or more intermediate nodes that are near neighbors to each other.

Definition 3 A group $\mathcal{S}_j \in \mathfrak{N}$ of UAVs, where $|\mathfrak{N}|$ is the number of deployed UAVs in a swarm, is strongly-connected if any UAV $n_j \in \mathcal{S}_j$ has a path with one or more hops to any other UAV $n_k \in \mathcal{S}_j$.

Definition 4 For $\mathcal{S}_j \in \mathfrak{N}$ defined in Definition 3, if $|\mathcal{S}_j| = |\mathfrak{N}|$, the swarm is connected.

Definition 5 A group $\mathcal{S}_j$ of strongly-connected UAVs is disconnected from the swarm if $|\mathcal{S}_j| < |\mathfrak{N}|$.

Now, let us present the following lemma stating that, when UAVs operating as a swarm are guided by our EFC, the swarm will be not partitioned by a UAV getting disconnected from it.

Lemma 1 *A single* UAV, *operating as a member of a swarm, does not get disconnected from the swarm if its movements are governed by* EFC.

Proof Let us first show that EFC will not select a location that disconnects a UAV n_i from the swarm. Based on Eq. 1, a candidate position for n_i which results in $|\mathcal{N}_i(t)| = 0$ (i.e., isolating n_i from its neighbors) would produce a fitness $\mathcal{F}_i$ that is prohibitively large, and, hence this candidate location will be excluded from further consideration. This eliminates network partitioning by a single node wandering away from the swarm. Recall that parameter $\theta(t)$, defined in Eq. (4), prevents n_i from taking steps that are too large to disconnect it from its neighbors by moving away from each other. At initial stages of deployment, UAVs are close to each other and need to disperse quickly, and, hence, $\theta(t)$ is kept close to its lower limit (e.g., $\theta(t) \geq 2 + \epsilon$, for a small ϵ). For the worst case, Eq. (4) states that $R_m(t) < \left(R_c - d(n_i, n_j^c)\right)/\theta(t)$ for $\theta(t) > 2$, which prevents n_i from obtaining a location farther than R_c apart from its closest neighbor n_j^c even if n_i and n_j^c simultaneously move in opposite directions at time $(t+1)$. As time progresses and network topology moves toward a uniform distribution over a mobile EM source, each UAV takes smaller steps governed by increased values of $\theta(t)$ to provide more precision on its movements at time $(t+1)$, which even further prohibits separation from the swarm. □

Lemma 1 states that EFC will prohibit n_i to be disconnected from the swarm. Let us now introduce the following lemma showing that our non-cooperative game will not allow a UAV to disconnect from the swarm.

Lemma 2 *A single* UAV, *operating as a member of a swarm, does not get disconnected from the swarm if its movements are governed by* EFC *and non-cooperative game* NCDG.

Proof NCDG sets up non-cooperative games between a UAV n_i and its near neighbors $n_j, \forall n_j \in \mathcal{N}_i(t)$, where possible strategies to select positions to move for each player are generated by EFC. Any strategy profile $S \in \Gamma_i(t)$ to be considered by NCDG will be based on the locations obtained using Eq. (1). As shown in Lemma 1, EFC produces candidate locations in generation Λ^L that keep n_i part of the swarm. Therefore, NCDG, together with EFC, will make movement decisions that will not disconnect n_i from the swarm. □

Recall in Eq. 2 that the value of parameter α can be adjusted such that when uniform distribution of UAVs is more important than tracking a mobile EM emitter, it is set as $\alpha \approx 0$. In such cases, as can be seen in Eqs. (1) and (2), even significant changes in EM signal strength will have marginal impact on movement decisions. Let us refer to this mode of operation, where the main objective is uniform distribution of UAVs, as *spreading mode*. For situations where zeroing-on a mobile EM transmitter or escaping its influence is pertinent, greater values of α should be preferred (i.e., $\alpha \approx 1$). We will call this mode of operation, where handling EM influence on movement decisions takes priority, *tracking mode*. Although in practice, spreading and tracking modes of operation overlaps, for the sake of simplicity, we will keep the formal analysis for swarm spreading and tracking modes separate in the rest of this section.

Note that Lemmas 1 and 2 proving that a single node does not get disconnected from a swarm under guidance of EFC and NCDG hold for UAVs operating as swarms in both spreading and tracking modes.

Definition 6 Total fitness of a UAV swarm, whose movements are governed by EFC and non-cooperative game NCDG, is defined at time t as $\mathcal{F}_{\mathfrak{N}}(t) = \sum_{i=1}^{\mathfrak{N}} \mathcal{F}_{n_i}(t)$, where $\mathcal{F}_{n_i}(t)$ is the best fitness selected for n_i at time t.

Let us first consider the case of $\alpha \approx 0$ in Eq. (2), emphasizing swarm spreading over impact of a mobile EM transmitter. Next lemma states that, in spreading mode, when fitness improves for a swarm, inter-nodal distance between UAVs increase and hence the swarm spreading improves.

Lemma 3 *In a swarm of* UAVs, *whose movements are governed by* EFC *and non-cooperative game* NCDG *and operating in spreading mode with* $\alpha \approx 0$, $\mathcal{F}_{\mathfrak{N}}(t+1) < \mathcal{F}_{\mathfrak{N}}(t)$ *implies that the* UAVs *in the swarm are spread farther apart from each other at time* $(t+1)$ *than at time* t.

Proof As can be seen in Eq. (1), smaller values of fitness for a UAV n_i implies that inter-nodal distance is increased between n_i and its neighbors. Therefore, if $\mathcal{F}_{\mathfrak{N}}(t+1) < \mathcal{F}_{\mathfrak{N}}(t)$ holds, it implies that the total inter-nodal distances for all UAVs in $\mathfrak{N}$ is increased, and hence, the swarm members are

spread farther apart a time $(t+1)$ compared to time t. □

Built on Lemmas 1 and 2, the next theorem shows that, in spreading mode, EFC combined with NCDG will consider candidate locations to improve payoff for a UAV n_i in its non-cooperative games with its neighbors. Under this guidance, actions of n_i promote network spreading while avoiding overcrowding with other swarm members.

Theorem 1 *In a swarm operating in spreading mode with $\alpha \approx 0$, a UAV guided by EFC and NCDG selects new locations to move based on its best response in non-cooperative games setup with its near neighbors, which encourages network spreading and avoids overcrowded neighborhoods.*

Proof NCDG running at n_i sets a non-cooperative game $\Gamma_i = \langle P, S, U \rangle$, where the players are n_i and its near neighbors (i.e., $P = \{n_i \cup \mathcal{N}_i(t)\}$). As presented in Eq. (5), NCDG will select a preferred strategy for n_i as response to the strategies of its rational neighbors, formulated in Eq. (6) as its best response $\mathcal{R}_i$.

A payoff for a strategy s_i is based on its fitness defined in Eq. (1), where, in a spreading mode, positions close to near neighbors are less preferable than farther ones. Due to term $(R_c - d(n_i, n_j))$ in Eq. (3), smaller (i.e., more preferable) values for fitness $\mathcal{F}_i$ will be generated for those positions. Suppose a candidate position n_i is $p_k \in \mathcal{N}_i(t)$. If p_k is also attractive to its near neighbors $n_j \in \mathcal{N}_i(t)$, n_i will consider another position, with possibly worse fitness than p_k, to move at time $(t+1)$. In this case, NCDG played by a rational player (i.e., a player that always picks strategy s_i over strategy s_j if $\mathcal{U}_i(s_i, \boldsymbol{s}_{-i}) < \mathcal{U}_i(s_j, \boldsymbol{s}_{-i})$ as defined in Eq. (5)) will decide on locations that the others will not go to, hence, giving incentives for locations closer to neighbors $\mathcal{N}_i(t)$.

We can state that a single UAV n_i does not disconnect from a swarm, as shown in Lemmas 1 and 2. We know that NCDG played at time t among n_i and $\mathcal{N}_i(t)$ would steer a selfish n_i farther apart from its neighbors at time $(t+1)$ and hence increasing $\mathcal{F}_{\mathfrak{N}}(t+1)$ for $\forall n_i \in \mathfrak{N}$. Since better total fitness for a swarm implies improved spread as shown in Lemma 3, we can conclude that actions of n_i guided by EFC and NCDG would promote network spreading while avoiding overcrowded neighborhoods. □

After showing that EFC and NCDG working together promote spreading of swarm members by Theorem 1, the following theorem states that, when operating in spreading mode, they lead to a uniform distribution, where the distance among the pairs of UAVs is approximately R_c.

Theorem 2 *In a swarm operating in spreading mode with $\alpha \approx 0$, EFC and NCDG guide UAVs toward a uniform distribution, where $d(n_i, n_j) \approx R_c$ for $\forall n_i, n_j \in \mathcal{N}_i(t)$ pairs.*

Proof As spreading mode of operation continues in a swarm, a UAV will decrease the value of $\theta(t)$ parameter defined in Eq. (4) starting from v to approach its lower bound of 2. From Eqs. (1) and (3), this decrease causes the distance between pairs of UAVs approach R_c. Therefore, inter-nodal distance in a swarm approaches a uniform distribution with the amount of R_c units between pairs. □

Definition 7 For a UAV $n_i \in \mathfrak{N}$ at time t, a set of neighbors of near neighbors of n_i, denoted as $\mathcal{N}_i^2(t)$, is defined as a group of UAVs such that for any $n_j \in \mathcal{N}_i^2(t)$, n_i and n_j are either near neighbors (i.e., $n_j \in \mathcal{N}_i(t)$) or there exists a communication path between n_i and n_j with exactly one intermediate node.

For a given n_i, information needed for computing $\mathcal{N}_i^2(t)$ can be obtained at each $n_j \in \mathcal{N}_i(t)$ in the neighborhood by broadcasting a heartbeat message including its near neighbor information $\mathcal{N}_j(t)$ in addition to its location and RSS reading at time t.

Definition 8 Given two subsets of UAVs $\mathcal{T}_i, \mathcal{T}_j \subset \mathfrak{N}$, $\mathcal{T}_i$ and $\mathcal{T}_j$ partition the swarm if $\mathcal{T}_i \cap \mathcal{T}_j = \emptyset$ and $\mathcal{T}_i \cup \mathcal{T}_j = \mathfrak{N}$.

Let us now present the following theorem stating that a UAV guided by EFC and NCDG does not allow for a swarm to be partitioned.

Theorem 3 *In a swarm operating in spreading mode with $\alpha \approx 0$, given two subsets of UAVs $\mathcal{T}_i$ and $\mathcal{T}_j$, where $\mathcal{T}_i, \mathcal{T}_j \subset \mathfrak{N}$, EFC and NCDG do not let the UAVs in $\mathcal{T}_i$ and $\mathcal{T}_j$ partition the swarm at time $(t+1)$ (i.e., $\mathcal{T}_i \cap \mathcal{T}_j = \emptyset$ and $\mathcal{T}_i \cup \mathcal{T}_j = \mathfrak{N}$), iff each UAV $n_k \in \mathfrak{N}$ possesses $\mathcal{N}_k^2(t)$ information at time t.*

Proof *(Sketch)* First let us show that if $n_i \in \mathcal{T}_i$ and $n_j \in \mathcal{T}_j$ do not possess $\mathcal{N}_i^2(t)$ and $\mathcal{N}_j^2(t)$ information at time t, respectively, it is possible that $\mathcal{T}_i$ and $\mathcal{T}_j$ may be disconnected at time $(t+1)$. Suppose that n_i and n_j are the only near neighbors connecting $\mathcal{T}_i$ and $\mathcal{T}_j$. Further suppose that n_i finds a position to improve its fitness that requires it to move the maximum allowed distance of $(R_c/2)$ units away (as defined in Eq. (4)) such that it will still maintain $\mathcal{N}_i(t+1) \neq 0 \in \mathcal{T}_i$. While n_i makes this movement decision, at the same time, n_j may find its best position to move $(R_c/2)$ units away, but in the opposite direction of n_i, while still maintaining $\mathcal{N}_j(t+1) \neq 0 \in \mathcal{T}_j$. In this case, it is possible that the total distance between n_i and n_j at time $(t+1)$ may be $d(n_i, n_j) > R_c$. For example, if they were $(R_c - \epsilon)$ units away from each other at time t (for a small value of ϵ) they will be

disconnected at time $(t+1)$. Therefore, without $\mathcal{N}_i^2(t)$ information in n_i and $\mathcal{N}_j^2(t)$ in n_j, while maintaining their own set of near neighbors, n_i and n_j may be able to disconnect $\mathcal{T}_i$ and $\mathcal{T}_j$ and hence partition the swarm if they were the only near neighbors connecting $\mathcal{T}_i$ and $\mathcal{T}_j$.

Now let us show that with $n_i \in \mathcal{T}_i$ and $n_j \in \mathcal{T}_j$ having $\mathcal{N}_i^2(t)$ and $\mathcal{N}_j^2(t)$ information at time t, respectively, it is not possible that $\mathcal{T}_i$ and $\mathcal{T}_j$ will be disconnected at time $(t+1)$. Suppose n_i and n_j consider moving $(R_c/2)$ units away from each other in opposite directions, while maintaining $\mathcal{N}_i(t+1) \neq 0 \in \mathcal{T}_i$. In this case, n_i will be aware of the fact that n_j is considering to make such a move which would partition the swarm, and, therefore, will avoid taking that step (this type of situations can be incorporated into the payoff function by having a lower payoff assigned to them by Eq. (5)). Similarly, n_j and other members will avoid such actions that may partition the swarm.

Therefore, in a swarm operating in spreading mode with $\alpha \approx 0$, EFC and NCDG do not let $\mathcal{T}_i$ and $\mathcal{T}_j$ partition the swarm *iff* each UAV $n_k \in \mathfrak{N}$ possesses $\mathcal{N}_k^2(t)$ information at time t. □

Let us now consider tracking mode of operation with $\alpha \approx 1$ in Eq. (2), emphasizing the impact of an EM transmitter on swarm actions. The following lemma states that, when a swarm is zeroing-on a mobile EM transmitter, EFC combined with NCDG will guide the UAVs such that they approach the mobile EM source and follow it.

Lemma 4 *A swarm operating in tracking mode with $\alpha \approx 1$, a single* UAV, *whose movements are guided by* EFC *combined with non-cooperative game* NCDG, *is capable of following a mobile* EM *source.*

Proof As given in Eq. (2), selection of $\alpha \approx 1$ will increase the swarm agility toward following an EM source based on the measurements of received signal strength from the transmitter. Consecutive decreasing RSS values imply that the distance between the EM source and n_i is increasing (either by moving opposite directions or EM transmitter moving away faster than n_i following it). Similarly, if there is an increase in consecutive RSS values in time, this implies that either UAV or the transmitter (or both) are moving toward each other. UAV n_i uses this information to create an EM heatmap of its surroundings using Eq. (7).

In tracking mode of operation, if n_i needs to zero-in on a mobile EM source, candidate position p_i with higher $\text{RSS}(t, p_i)$ value at time t will be preferable to other candidates with lower values as presented in Eqs. (1) and (2). Therefore, EFC combined with non-cooperative game NCDG will guide each UAV to zero-in and follow a mobile EM transmitter. □

Similarly, in tracking mode, if the goal of a swarm is to avoid a mobile EM source, candidate positions with lower $\text{RSS}(t, p_i)$ values will be given priority in Eqs. (1) and (2). Therefore, we can state the following corollary to Lemma 4.

Corollary 1 *A swarm operating in tracking mode with $\alpha \approx 1$, a single* UAV, *whose movements are guided by* EFC *combined with non-cooperative game* NCDG, *is capable of avoiding a mobile* EM *source.*

At this point, we present the following corollary to Theorem 1 stating that a swarm operating in tracking mode will follow a mobile EM transmitter. In tracking mode, non-cooperative game NCDG played at time t among n_i and and its near neighbors $\mathcal{N}_i(t)$ would steer a selfish n_i closer to a mobile EM source at time $(t+1)$ by preferring candidate positions with higher $\text{RSS}(t, p_i)$ values.

Corollary 2 *In a swarm operating in tracking mode with $\alpha \approx 1$, a* UAV *guided by* EFC *and* NCDG *selects new locations to move based on its best response in non-cooperative games setup with its near neighbors such that the swarm follows a mobile* EM *source.*

Similarly, we introduce another corollary to Theorem 1 for a swarm operating in tracking mode, where swarm objective is to avoid a mobile EM source. In this case, NCDG would incentivize a selfish n_i to move farther away from the EM source at time $(t+1)$ by giving positions with lower $\text{RSS}(t, p_i)$ values higher priority.

Corollary 3 *In a swarm operating in tracking mode with $\alpha \approx 1$, a* UAV *guided by* EFC *and* NCDG *selects new locations to move based on its best response in non-cooperative games setup with its near neighbors such that the swarm avoids a mobile* EM *source.*

The following corollary to Theorem 3 states that in tracking mode, where the objective is either to zero-in on a mobile EM transmitter or to avoid it, a UAV guided by EFC and NCDG does not allow for a swarm to be partitioned.

Corollary 4 *In a swarm operating in tracking mode with $\alpha \approx 1$, given two subsets of* UAVs *$\mathcal{T}_i$ and $\mathcal{T}_j$, where $\mathcal{T}_i, \mathcal{T}_j \subset \mathfrak{N}$,* EFC *and* NCDG *do not let the* UAVs *in $\mathcal{T}_i$ and $\mathcal{T}_j$ partition the swarm at time $(t+1)$ (i.e., $\mathcal{T}_i \cap \mathcal{T}_j = \emptyset$ and $\mathcal{T}_i \cup \mathcal{T}_j = \mathfrak{N}$), iff each* UAV *$n_k \in \mathfrak{N}$ possesses $\mathcal{N}_k^2(t)$ information at time t.*

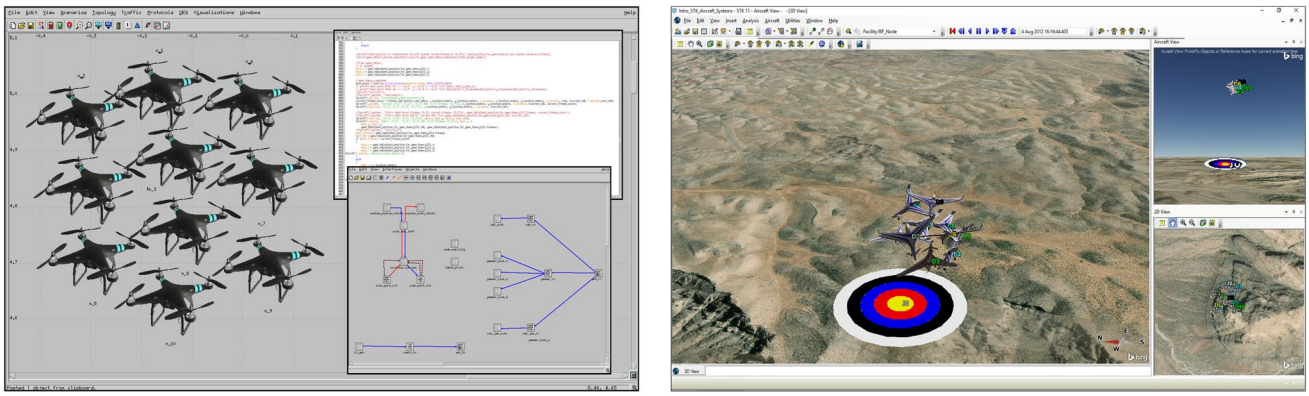

Fig. 4 Simulation of UAV swarms: **a** OPNET Modeler environment for communication and movement capabilities of autonomous UAV swarms, **b** STK visualization for deployment of a UAV swarm over a realistic terrain

5 Simulation experiments

In the previous section, we present a formal analysis showing that EFC and NCDG can guide UAVs operating as a swarm in either spreading or tracking modes to maintain a connected MANET, promote a uniform network spreading. In this section, we present the results of a set of simulation experiments run in OPNET Modeler using realistic experiment setups to verify the results of formal analysis.

5.1 Simulation environment

We implemented our EFC and NCDG flight control algorithms in OPNET Modeler[32] that let us simulate wireless communication and signal propagation characteristics in realistic settings. In our experiments, we set radio frequency, antenna type and transmission power parameters for each UAV to facilitate the communication range R_c needed by different swarm configurations used throughout the experiments. In an effort to simulate real-life conditions as much as possible, OPNET Modeler also allows for specifying encoding type, data rate and packet size for each network interface to best mimic errors that could be introduced during a transmission. In our experiments, without loss of generality, we simulated a mobile EM source to propagate radio signals on a different frequency band than the one used by UAVs for broadcasting their heartbeat messages. UAVs are equipped with radio receivers capable of measuring RSS at the frequency used by an EM transmitter. Each autonomous UAV makes independent movement decisions using real-life earth coordinates and EM signal landscape of dynamically changing environments.

Figure 4a shows a sample screen-capture from OPNET during an experiment simulating communication and movement operations of swarms of autonomous UAVs maintaining MANET topology while operating in spreading and tracking modes. Overlapping top right pane of Fig. 4a depicts one of panes that are used for coding autonomous UAV decision making software modules implementing our EFC and NCDG algorithms and UAV movement parameters. Interaction among various simulated hardware components and communication and flight control modules are shown in the bottom right pane of Fig. 4a.

We employ Systems Tool Kit (STK)[43] to visualize the movements of UAV swarms over real 3D terrain maps. With the use of STK, our UAV swarm can fly above terrain maps that accurately model earth elevations in a specific deployment theatre. Figure 4b presents a screen capture from STK for a 3D visualization of a UAV swarm, where the mobile EM source is indicated as a target mark. In the perspective view of the main left pane, the EM source and a swarm of 10 UAVs overshadowing it from above are shown. The top right pane in Fig. 4b is a side-view of the swarm approaching the target. This view is typically used to determine altitude differences among UAVs and the EM source. The bottom right pane is the top-view observed from directly above the EM source to indicate the area over which UAVs operate.

5.2 Simulation setup

In our simulations experiments, each autonomous UAV independently determines its position to move by running our EFC and NCDG based flight control algorithms. UAVs in a swarm are not synchronized and do not rely on any prior information except an initial approximation of the location of the mobile EM transmitter. No other information about movement of mobile EM source is required by the UAVs when they are launched. We run simulation experiments for swarms with 5, 10, or 20 UAVs. UAVs in each of these swarms are assigned communication ranges of $R_c = 100\,\text{m}, 200\,\text{m}$ or $400\,\text{m}$. For simplicity and without loss of generality, UAVs in our simulation experiments have the same flight capabilities (e.g., they fly with maximum speed of 10 m/s) and the same

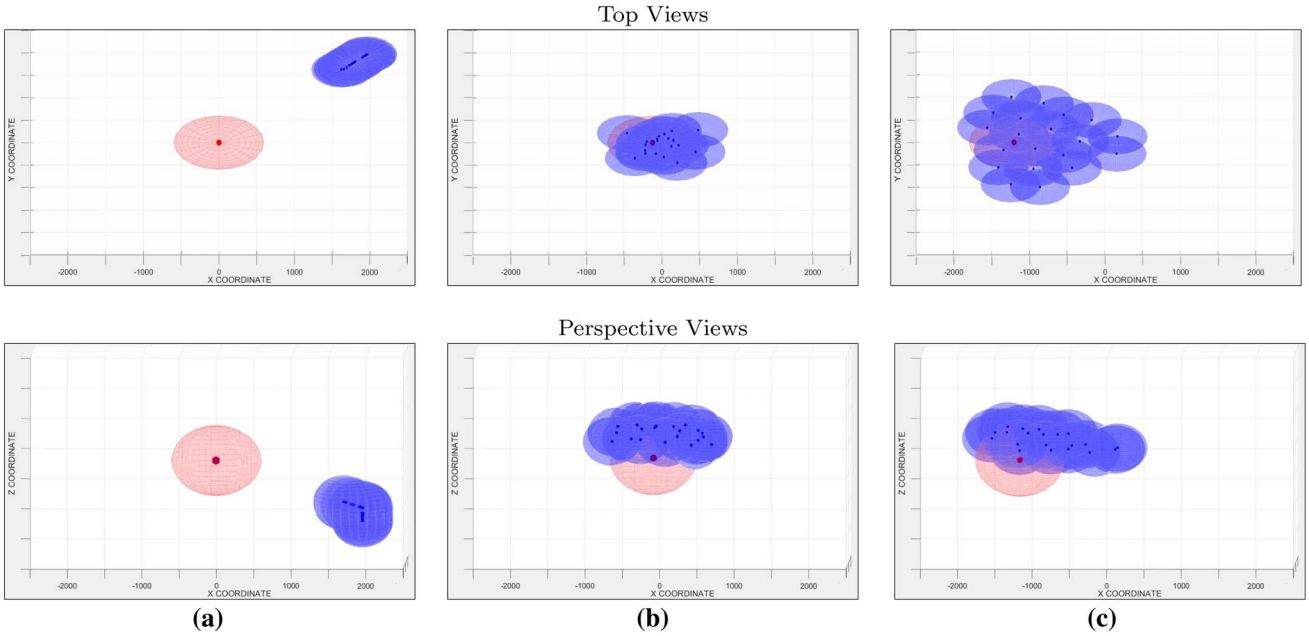

Fig. 5 OPNET simulation of a 20-UAV swarm: **a** at their entry to a mission theatre, **b** after the swarm forms a MANET over an initial location of a mobile EM emitter, **c** as the swarm tracks a mobile EM emitter

communication range R_c. Each UAV in move with six degrees of freedom, namely, forward and backward, up and down, left and right, and can rotate along each axis for yaw, pitch and roll adjustments.

In each experiment, UAVs are dispatched from a single entry point after which they form a MANET over an area of interest in a 5 km × 5 km theatre. A mobile EM interference source is initially placed at the center of the theatre, which flies with the intermittent speed of 2 m/s. The EM source starts moving at time $t = 5$ min and it relocates toward the left of the theatre for a duration of 30 min. Each swarm deployment was simulated as a 60-min mission, which then repeated 10 times with the same parameters and the results averaged to eliminate noise in the collected data.

We designed these simulation experiments to analyze the performance of different swarm configurations for their effectiveness in spreading and tracking modes of operations and their abilities to maintain MANET connectivity during missions.

Figure 5 shows a UAV swarm responding to unpredictable actions of a mobile EM transmitter that is depicted as a target mark. In the top view of Fig. 5a, a 20-UAV swarm is dispatched from the ground at the top right corner of the theatre. As can be seen in the perspective view of Fig. 5a, the UAVs first increase their elevation to avoid potential lower level ground obstacles and then begin to fly toward the EM transmitter. This type of deployment resembles realistic situations, where all dispatched UAVs know only the initial flight destination at the beginning and are launched from a single entry point outside of the mission theatre. After arriving at the initial location, UAVs start spreading to maximize area coverage over the EM source while maintaining network connectivity (Fig. 5b). When the EM transmitter moves from its initial location at the center of the deployment theatre to ≈ 1.2 km left of it (top view of Fig. 5c), swarm successfully zeros-in on the mobile source during the remainder of the experiment. As noted earlier, the UAVs do not have any knowledge about the actions of the mobile EM source.

5.3 Surface of the earth coverage

Surface of the earth coverage (SEC) is a metric for evaluating the effectiveness of UAV swarms in overshadowing a terrain of interest. In our experiments, SEC is defined as the ratio of the coverage achieved by the communication ranges of all UAVs to the ground area around a mobile EM emitter $A_{\text{EM}}(t)$ at time t. If the region is covered by more than one UAV, overlapped area is included in SEC calculations only once. Also, if the communication range of a UAV extends beyond $A_{\text{EM}}(t)$, only the part of its coverage that is within A_{EM} counts toward SEC metric. Let $\mathcal{A}_i(t)$ denote the 2D ground area covered by R_c of UAV n_i at time t. We define SEC for a swarm at time t as

$$\text{SEC}(t) = \frac{\bigcup_{n_i \in \mathfrak{N}} \mathcal{A}_i(t)}{A_{\text{EM}}(t)} \tag{8}$$

where $\bigcup$ represents the union of areas covered by $\forall n_i \in \mathfrak{N}$. SEC values close to 1 imply that the entire area $A_{\text{EM}}(t)$ is

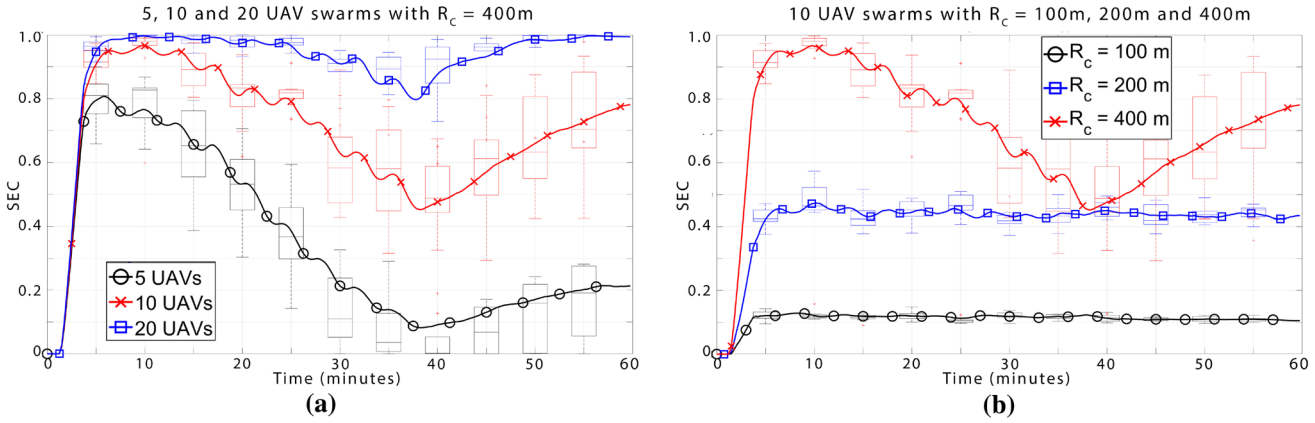

Fig. 6 Surface of the earth coverage for swarms guided by EFC and NCDG: **a** total number of UAVs $\mathfrak{N} = 20, 10$, and 5 with communication range $R_c = 400\,\text{m}$; and **b** 10-UAV swarm with communication ranges of $R_c = 400\,\text{m}, 200\,\text{m}$ and 100 m (note that the EM source starts moving at $t = 5\,\text{min}$, which initiates a drop in SEC for all cases, and stops moving at $t = 35\,\text{min}$, after which SEC starts to recover)

covered while smaller values indicate that some of the terrain around the mobile EM transmitter are not adequately monitored. Obtaining the highest possible SEC by mobile UAVs is one of the important goals for our flight control provided by EFC and NCDG algorithms.

We evaluate performance of swarms with 5, 10 and 20 UAVs and operating with different R_c values with respect to their abilities to maintain a high SEC throughout experiments. In our experiments, the area influenced by the signal transmitted from a mobile EM source $A_{\text{EM}}(t)$ is defined as $1\,\text{km} \times 1\,\text{km}$ square with the EM transmitter at its center. As the mobile EM source moves, the target area of A_{EM} that it defines also moves with it. Figure 6 displays the change in SEC throughout simulation experiments obtained by swarms of autonomous UAVs running EFC and NCDG algorithms to determine their moves as time progresses and the EM landscape changes. The outcomes in Fig. 6 are presented as boxplots, where the boxes indicate ranges containing 50% of the results and the whiskers are the minimum and maximum values for each measurement.

Figure 6a shows the SEC obtained by swarms with 5, 10 and 20 UAVs using a communication range of $R_c = 400\,\text{m}$. As anticipated, larger swarms are able to cover respectively wider areas than swarms with less UAVs. We can see in Fig. 6a that as the UAVs approach to the center of the theatre during the first minutes of the experiments, SEC keeps increasing until it reaches SEC of 0.80, 0.95 and 1.0 for swarms with 5, 10 and 20 UAVs, respectively. After the mobile EM transmitter starts moving away from its initial position at time $t = 5\,\text{min}$, SEC starts decreasing for all three swarm configurations, as autonomous UAVs need time to respond to the changes in EM landscape caused by the movement of the transmitter. As we can see in Fig. 6a, during the next 30 min of the experiments, swarms follow the mobile target, but slightly lag with their abilities to adequately overshadow the terrain of $A_{\text{EM}}(t)$ influenced by the mobile EM transmitter. Toward the end of the experiments, UAVs start restoring their respective SEC after the EM signal source stops moving, with less populated swarms needing more time to do so since they have to move farther to cover the same territory.

Figure. 6b shows SEC for 10-UAV swarms with varying communication ranges of $R_c = 100\,\text{m}, 200\,\text{m}$ and 400 m. As expected, swarms with longer communication ranges cover proportionately wider 2D areas than the ones with shorter ranges. We observe in Fig. 6b that the highest SEC measurements for all swarm configurations are obtained at approximately the same time (at $t \approx 6\,\text{min}$) in the experiments. Although better coverage is achieved by UAVs with wider communication ranges of R_c, SEC obtained by the swarm with $R_c = 400\,\text{m}$ degrades considerably when the EM transmitter starts to move at time $t = 5\,\text{min}$. This phenomena is attributed to the fact that, for large values of R_c, proportionally large drops happen in SEC initiated by even a small relocation of the mobile EM emitter. On the other hand, swarms with shorter communication ranges (i.e., $R_c = 100\,\text{m}$ and $200\,\text{m}$) can occupy the center of $A_{\text{EM}}(t)$ and, hence, have more time to react to any changes in the EM landscape before the area covered by them starts falling outside of $A_{\text{EM}}(t)$.

We can observe in Fig. 6 that SEC is directly proportional to both the number of UAVs in the swarm and the communication range of a UAV. However, we also observe that a decrease in swarm size or communication range R_c does not significantly reduce abilities of a swarm to adequately cover the terrain around the mobile EM source. Swarms with more UAVs need more time to react to the changes in EM landscape since there are more UAVs to properly spread over $A_{\text{EM}}(t)$. Based on simulation experiments, we can conclude that when a large area of a terrain needs to be overshadowed a swarm autonomous UAVs, it is better to keep the swarm size large with UAVs possessing greater ranges of R_c.

5.4 Tracking analysis

In this section we analyze performance of different swarm configurations guided by EFC and NCGD responding to changes in EM landscape due to mobility of an EM transmitter. Due to space restrictions in this paper and without loss of generality, in the simulation experiments presented in this section, we only focus on tracking mode with the goal of following a mobile EM transmitter. Although the main objective for the swarm is to zero-in on a mobile EM source, we could easily conduct a similar set of experiments, where NCGD gives incentives to positions with weaker signal strength, which would force a UAV to move away from the mobile EM source.

To determine efficiency of a swarm in following a mobile EM target, we compute distance $\mathcal{D}(t)$ between an EM transmitter position $p_{\text{EM}}(t)$ and the center of mass of a swarm $\mathcal{S}$ at time t, denoted as $\mathcal{C}_{\mathcal{S}}(t)$, that follows it throughout the experiments (i.e., from $t = 0$ until the end of each mission at $t = 60$ min) as

$$\mathcal{D}(t) = d\big(p_{\text{EM}}(t), \mathcal{C}_{\mathcal{S}}(t)\big) \tag{9}$$

When the center of a swarm is directly above the EM source, then $\mathcal{D}(t) \approx 0$. Larger values of $\mathcal{D}(t)$ indicate that the centroid for the swarm is shifted with respect to the location of an EM transmitter at time t and, hence, the area around it will not be adequately covered.

Figure 7 shows $\mathcal{D}(t)$ values for swarms zeroing-in on a mobile EM source with 5, 10 and 20 UAVs and the communication ranges of $R_c = 100$ m, 200 m and 400 m. As in all of our simulation experiments, the EM transmitter starts to move at time $t = 5$ min and keeps changing its location until $t = 35$ min. Only an approximate initial position of the EM source is known to UAVs at the time of deployment. Each autonomous UAV makes its movement decisions based on spatial and temporal changes in EM landscape around itself by obtaining EM heatmaps using Voronoi tessellations of the area around it [as presented in Eq. (7)].

Figure 7a shows changes in $\mathcal{D}(t)$ for swarms with 5 UAVs using $R_c = 100$ m, 200 m and 400 m operating in tracking mode by zeroing-in on a mobile EM source. We can observe in Fig. 7a that when the EM transmitter initiates its move at $t = 5$ min, the distance $\mathcal{D}(t)$ for each swarm starts increasing with a slightly delayed response to the EM landscape changes. As experiment progresses, each swarm regains its adequate coverage of the center of A_{EM} as can be seen in Fig. 7a by the decreasing $\mathcal{D}(t)$ values, after the mobile EM stops at $t = 35$ min. The swarms with communication ranges of $R_c = 100$ m and 200 m are able to successfully recenter around the EM transmitter by the end of the simulation experiments. We can observe that, for swarms with 5 UAVs, $R_c = 200$ m is the preferable communication range compared to $R_c = 100$ m and 400 m since

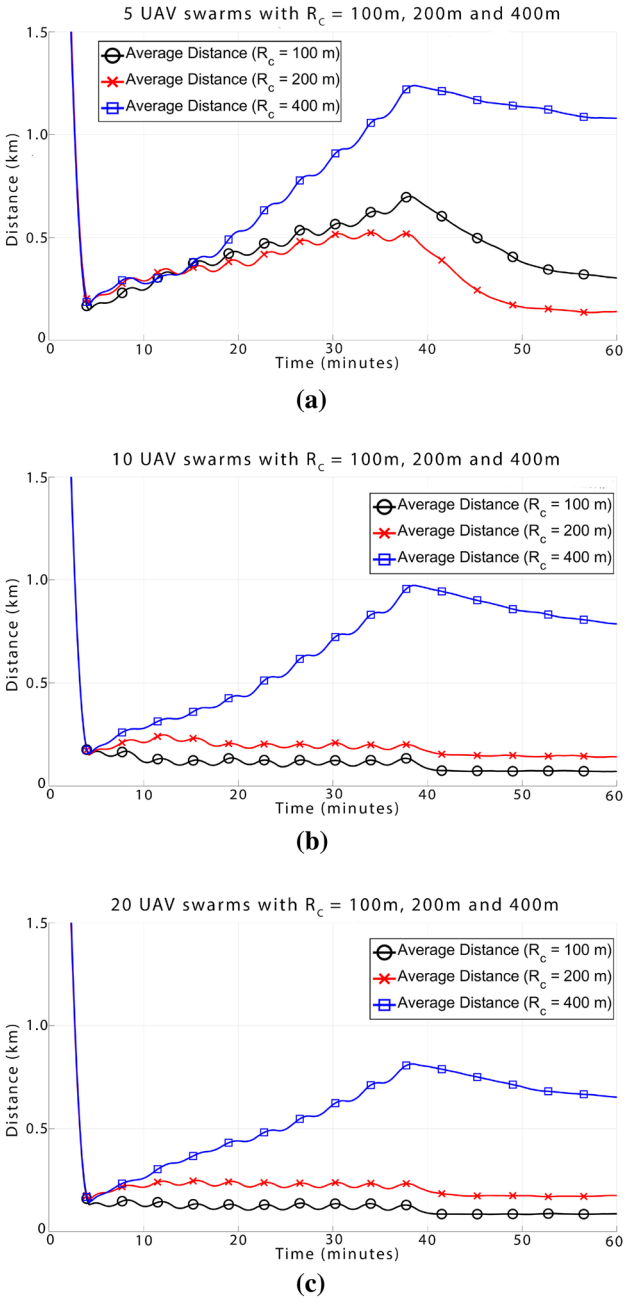

Fig. 7 Distance from a mobile EM source to center of mass of swarms with $R_c = 100$ m, 200 m and 400 m and **a** 5 UAVs, **b** 10 UAVs, **c** 20 UAVs

it recovers faster than the others for the EM transmitter moving with a slower speed than the top speed of UAVs (in these experiments, they are selected as 2 m/s and 10 m/s, respectively). Larger values of $\mathcal{D}(t)$ observed in Fig. 7a for the 5-UAV swarm using $R_c = 400$ m can be attributed to the fact that the swarm following the movements of an EM target has to cover greater distances to obtain a uniformly distributed UAV topology compared to the swarms with shorter R_c ranges (i.e., inter-nodal distance for UAVs will

be approximately 400 m, whereas they are 100 m and 200 m for the other swarms).

In Fig. 7b, the $\mathcal{D}(t)$ values are shown for the swarms with 10 UAVs and $R_c = 100\,\text{m}, 200\,\text{m}$, and 400 m, each following a mobile EM source. We can observe that more dense swarms (i.e., smaller ranges of R_c among UAVs) are more agile in centering over A_{EM}. For example, for $R_c = 100\,\text{m}$, the swarm keeps $\mathcal{D}(t) \approx 0$ throughout the experiment, whereas for $R_c = 400\,\text{m}$ $\mathcal{D}(t)$ increases when the emitter moves from $t = 5$ min until it stops at $t = 35$ min to a value of $\mathcal{D}(t) \approx 1$ km before it regains its centering over A_{EM} with $\mathcal{D}(t) \approx 750$ m at the end of the experiment.

We repeat the same experiments for larger swarms with 20 UAVs. In Fig. 7c, we display $\mathcal{D}(t)$ values for $R_c = 100\,\text{m}, 200\,\text{m}$, and 400 m. Consistent with the previous results, smaller communication ranges provide more agility than sparser swarms (i.e., swarms using $R_c = 400\,\text{m}$), which need more time to respond to the changes in the EM landscape.

Based on $\mathcal{D}(t)$ values displayed in Fig. 7a–c, we can conclude that more populated swarms tend to be more agile in responding to unpredictable mobility of an EM source. For example, at the end of an experiment, for $R_c = 400\,\text{m}$ 5-UAV swarms have $\mathcal{D}(t) \approx 1\,\text{km}$, compared to 10- and 20-UAV swarms with $\mathcal{D}(t) \approx 750\,\text{m}$ and 600 m, respectively.

5.5 Connectivity analysis

One of the important performance metrics for a MANET is its ability to maintain connectivity among its mobile nodes during an operation. As part of the evaluation of our EFC and NCDG algorithms, we monitor the connectivity of the MANET that the UAVs of a swarm form throughout experiments. Similar to the coverage and tracking experiments, swarm configurations with 5-, 10- and 20-UAVs using communication ranges of $R_c = 100\,\text{m}, 200\,\text{m}$, and 400 m are deployed for the connectivity analysis. After being launched from a single entry point outside of the mission theatre, UAVs increase their elevation to avoid ground obstacles and fly toward the initial approximate position of an EM transmitter. Upon arrival at the theatre, UAVs form a MANET, which will be monitored for connectivity among UAVs throughout experiments. As previously stated, each experiment is repeated 10 times to avoid noise in the collected results.

In Fig. 8a, the average number of connected components in a MANET over time for 5-UAV swarms is presented for $R_c = 100\,\text{m}, 200\,\text{m}$, ans 400 m. We observe that the swarms with small populations (i.e., $|\mathfrak{N}| = 5$ may get partitioned sporadically, especially after the EM source starts moving and the swarm initiates its tracking operation. Swarms with $R_c = 100\,\text{m}$ and 200 m regain and keep their MANET connectivity for the latter half of experiments. However, sparse

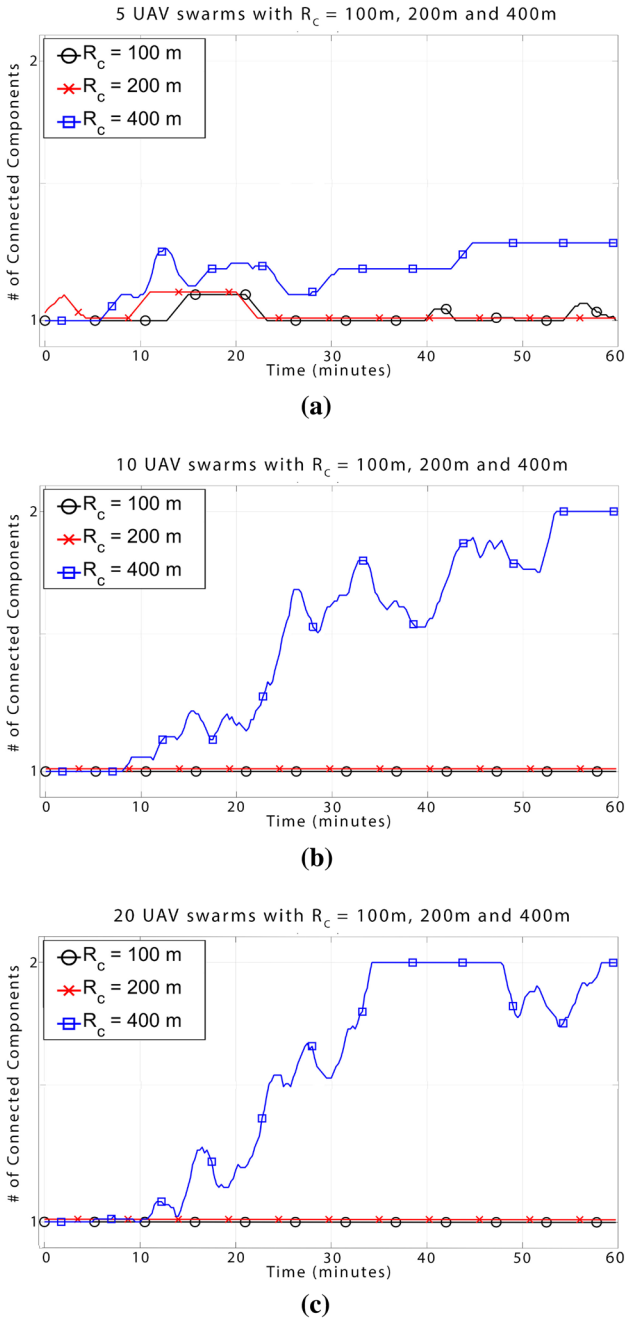

Fig. 8 Number of strongly connected components in swarms using $R_c = 100\,\text{m}, 200\,\text{m}$, and 400 m as they track a mobile EM target

swarms (i.e., $R_c = 400\,\text{m}$ and $|\mathfrak{N}| = 5$) struggle with keeping MANET connected until the end.

In Fig. 8b, we repeat the connectivity experiments with swarm sizes of 10-UAVs. In for these swarms, $R_c = 100\,\text{m}$ and 200 m ensure a fully-connected MANET, whereas UAVs with $R_c = 400\,\text{m}$ start losing connectivity after EM source starts moving and never regains it back. Experiments with 20-UAVs as shown in Fig. 8c indicate similar behavior that UAVs with longer communication ranges (i.e., $R_c = 400\,\text{m}$) lead to

partitioning of the swarm when tracking an EM source and that swarms using smaller communication ranges stay consistently connected.

Connectivity experiments shown in Fig. 8a–c indicate that for all realistic deployments of swarms $R_c = 100$ m and 200 m are preferred to longer communication ranges when connectivity is crucial for a given application. On the other hand, when swarms operate with longer communication ranges providing much larger surface coverage, they may experience network partitioning in zeroing-on unpredicatably moving EM sources. As a result of successful guidance provided by EFC and NCDG algorithms, size of swarms do not have an impact on MANET connectivity regardless of spreading and tracking mode of swarm operation.

6 Multiple EM transmitters

Our flight control algorithms, namely evolutionary flight control by EFC and non-cooperative game based decision making by NCDG, are presented for a single mobile EM source. EFC and NCDG are shown to handle tracking or avoiding a mobile EM emitter based on requirements of an application.

In the presence of multiple EM sources, the flight control and tracking becomes substantially more challenging. If the EM emitters are operating using the same frequency band, the Voronoi tessellations computed as in Eq. (7) can adequately address their cumulative impact on a UAV as follows. In this case, the RSS measured in a neighborhood reflects their cumulative effect from these multipe EM sources. Based on the spatial distribution of the EM sources in a theatre, a swarm of autonomous UAVs may have to split to handle such multiple emitters. EFC and NCDG algorithms presented in this paper are expected to handle these multiple sources with small modifications to the fitness and payoff functions given in Eqs. (1)–(6).

If, on the other hand, the multiple EM emitters operate on different frequency bands, there will be a different EM heatmap generated for each of the frequency bands. Handling multiple and different frequency bands requires payload augmentations in UAVs for ongoing monitoring of those channels. For $\mathcal{K}$ different EM sources, each operating in frequency f_k, $\forall k \in \mathcal{K}$, we need to compute a different weight factor $\gamma_k(t, p_i)$ to be used in the fitness function. Equations (1) and (2) must be modified as follows:

$$\mathcal{F}_{i,k} = \begin{cases} \gamma_k(t,p_i) \sum_{j=1}^{\mathcal{N}_i(t)} D_{ij} & \text{if } |\mathcal{N}_i(t)| \geq 1 \\ \mathcal{M}_c & \text{otherwise} \end{cases} \tag{10}$$

$$\gamma_k(t,p_i) = (1+\epsilon) - \left(\frac{\text{RSS}_k(t+1,p_i) - \text{RSS}_k(t,p_i^{min})}{\text{RSS}_k(t,p_i^{max}) - \text{RSS}_k(t,p_i^{min}) + \epsilon} \right) \tag{11}$$

In Eq. (10), $\mathcal{F}_{i,k}$ reflects the fitness for candidate positions calculated by a UAV n_i when it is handling an EM emitter with frequency f_k. Similarly, weight $\gamma_k(t, p_i)$ in Eqs. (10) and (11) incorporates changes in EM landscape for frequency f_k at time t with RSS_k are the signal strength measurements for f_k.

Assignment of UAVs to each EM frequency f_k is a different class of problem and is beyond the scope of this paper. Suppose that groups of UAVs can be assigned to different EM frequencies prior to their deployment. If this assumption holds, each UAV group will form a separate swarm responding to the EM emitter operating in frequency f_k under the guidance of our EFC and NCDG algorithms. Extension of our research work will include modification of fitness and game models to handle multiple and simultaneous mobile EM emitters.

7 Concluding remarks

In this paper, we present AI and GT based near real-time flight control algorithms for swarm of autonomous UAVs based only on local spatial, temporal and EM information. Each UAV runs our flight control algorithms to position itself such that the swarm maintains a connected MANET and a uniform asset distribution over an area of interest, while tracking unpredictable movements of an EM transmitter. We formally analyzed our algorithms to show that they can guide a swarm to maintain a connected MANET, promote a uniform network spreading, and avoid overcrowding with other swarm members. We also prove that swarms of autonomous UAVs guided by our algorithms can maintain MANET connectivity and simultaneously lead a swarm to follow or avoid an EM transmitter. We conduct simulation experiments in OPNET Modeler to verify the results of our formal analysis. Our algorithms rely only on limited near neighbor communication without any central controllers, UAV synchronization mechanisms or pre-planned set of actions. They are good candidates for civilian and military applications that require agile responses to the changes in dynamic environments for tasks such as detection, localization and tracking mobile EM transmitters.

Future extensions of this research include introduction of multiple and independent EM sources operating in environments with fixed and mobile obstacles. We plan to show that our algorithms provide near real-time flight control for autonomous UAVs in spite of loss of assets, attacks on communications channels and presence of malicious neighbors.

Acknowledgements This research is supported by a Grant from US Army Combat Capabilities Development Command (CCDC)—Command Control Communication Computers Cyber Intelligence Surveillance Reconnaissance (C5ISR) Center D01 W911SR-14-2-0001-0014. The contents of this document represent the views of the authors and are not necessarily the official views of, or endorsed by, the US Government, Department of Defense, Department of the Army or US Army CCDC C5ISR Center.

References

1. Altshuler Y, Pentland A, Bruckstein A (2018) Swarms and network intelligence in search. Springer, Berlin
2. Alzenad M, El-Keyi A, Lagum F, Yanikomeroglu H (2017) 3-D placement of an unmanned aerial vehicle base station (UAV-BS) for energy-efficient maximal coverage. IEEE Wirel Commun Lett 6(4):434–437
3. Bardhan R, Bera T, Sundaram S (2017) A decentralized game theoretic approach for team formation and task assignment by autonomous unmanned aerial vehicles. In: International conference on unmanned aircraft systems (ICUAS), pp 432–437
4. Bucaille I, Hethuin S, Rasheed T, Munari A, Hermenier R, Allsopp S (2013) Rapidly deployable network for tactical applications: aerial base station with opportunistic links for unattended and temporary events absolute example. In: IEEE military communications conference (MILCOM), pp 1116–1120
5. Carvalho J, Jucá M, Menezes A, Olivi L, Marcato A, dos Santos A (2017) Autonomous UAV outdoor flight controlled by an embedded system using Odroid and ROS. Controlo 2016:423–437
6. Cetin O, Yilmaz G (2016) Real-time autonomous UAV formation flight with collision and obstacle avoidance in unknown environment. J Intell Robot Syst 84(1–4):415–433
7. Cho J, Kim J (2018) Performance comparison of heuristic algorithms for UAV deployment with low power consumption. In: International conference on information and communication technology convergence (ICTC). IEEE, New York, pp 1067–1069
8. Clark A, Sun K, Bushnell L, Poovendran R (2015) A game-theoretic approach to IP address randomization in decoy-based cyber defense. In: International conference on decision and game theory for security, pp 3–21
9. Das S, Tripathi S (2018) Adaptive and intelligent energy efficient routing for transparent heterogeneous ad-hoc network by fusion of game theory and linear programming. Appl Intell 48(7):1825–1845
10. Davis D, Chung T, Clement M, Day M (2016) Consensus-based data sharing for large-scale aerial swarm coordination in Lossy communications environments. In: International conference on intelligent robots and systems (IROS), pp 3801–3808
11. Du Q, Faber V, Gunzburger M (1999) Centroidal Voronoi tessellations: applications and algorithms. SIAM Rev 41(4):637–676
12. Eldosouky AR, Ferdowsi A, Saad W (2019) Drones in distress: a game-theoretic countermeasure for protecting UAVs against GPS spoofing. IEEE Internet Things J 7:2840–2854
13. Elhoseny M, Yuan X, Yu Z, Mao C, El-Minir H, Riad A (2015) Balancing energy consumption in heterogeneous wireless sensor networks using genetic algorithm. IEEE Commun Lett 19(12):2194–2197
14. Findeis D, Balchanos M, Vachtsevanos G, Mavris D (2019) Modeling and simulation of UAV swarm formation control in response to wind gusts. In: AIAA Scitech 2019 Forum, p 1571
15. Fudenberg D, Tirole J (1991) Game theory. The MIT Press, New York
16. Garapati K, Roldán J, Garzón M, del Cerro J, Barrientos A (2017) A game of drones: game theoretic approaches for multi-robot task allocation in security missions. In: Iberian robotics conference, pp 855–866
17. Gundry S, Zou J, Urrea E, Sahin C, Kusyk J, Uyar M (2012) Analysis of emergent behavior for GA-based topology control mechanism for self-spreading nodes in MANETs. Adv Intell Model Simul Artif Intell Based Models Tech Scalable Comput 422:155–183
18. Gundry S, Zou J, Uyar M, Sahin C, Kusyk J (2015) Differential evolution-based autonomous and disruption tolerant vehicular self-organization in MANETs. Ad Hoc Netw 25(B):454–471
19. Ji Z, Liu K (2008) Multi-stage pricing game for collusion-resistant dynamic spectrum allocation. IEEE J Sel Areas Commun 26(1):182–191
20. Karaboga D, Okdem S, Ozturk C (2012) Cluster based wireless sensor network routing using artificial bee colony algorithm. Wireless Netw 18(7):847–860
21. Kusyk J, Sahin C, Zou J, Gundry S, Uyar M, Urrea E (2013) Game theoretic and bio-inspired optimization approach for autonomous movement of MANET nodes. In: Zelinka I, Snášel V, Abraham A (eds) Handbook of optimization. Intelligent systems reference library, vol 38. Springer, Berlin, Heidelberg
22. Kusyk J, Urrea E, Sahin C, Uyar M (2012) Game theory and genetic algorithm based approach for self positioning of autonomous nodes. Int J Ad Hoc Sensor Wirel Netw 16:93–118
23. Kusyk J, Uyar M, Ma K, Ma K, Budhu K, Samoylov E, Plishka J, Bertoli G, Boksiner J (2019) Game theory and biology inspired flight control for autonomous UAVs operating in contested environments. In: 40th IEEE Sarnoff symposium, pp 1–6
24. Kusyk J, Uyar M, Ma K, Ma K, Plishka J, Bertoli G, Boksiner J (2019) AI and game theory based autonomous UAV swarm for cyber security. In: IEEE military communications conference (MILCOM), pp 1–6
25. Kusyk J, Uyar M, Sahin C (2018) Survey on evolutionary computation methods for cyber security of mobile ad hoc networks. Evol Intell 10:95–117
26. Kusyk J, Zou J, Gundry S, Sahin C, Uyar M (2013) Performance metrics for self-positioning autonomous MANET nodes. J Cybersecurity Mob 2:151–173
27. Mahler RP (2007) Statistical multisource-multitarget information fusion, vol 685. Artech House, Norwood
28. Merwaday A, Guvenc I (2015) UAV assisted heterogeneous networks for public safety communications. In: Wireless communications and networking conference workshops (WCNCW), pp 329–334
29. Mousavi S, Afghah F, Ashdown J, Turck K (2019) Use of a quantum genetic algorithm for coalition formation in large-scale UAV networks. Ad Hoc Netw 87:26–36
30. Mozaffari M, Saad W, Bennis M, Debbah M (2016) Unmanned aerial vehicle with underlaid device-to-device communications: performance and tradeoffs. IEEE Trans Wirel Commun 15(6):3949–3963
31. Nash J (1950) Equilibrium points in n-person games. Proc Natl Acad Sci USA 36:48–49
32. OPNET Modeler, Riverbed Tech., Inc. https://www.riverbed.com/products/steelcentral/opnet.html/. Accessed 01 Nov 2019
33. Reina D, Ruiz P, Ciobanu R, Toral S, Dorronsoro B, Dobre C (2016) A survey on the application of evolutionary algorithms for mobile multihop ad hoc network optimization problems. Int J Distrib Sensor Netw 12:2082496
34. Sahin C, Gundry S, Uyar M (2012) Markov chain analysis of self-organizing mobile nodes. J Intell Robot Syst 67(2):133–153
35. Sampedro C, Bavle H, Sanchez-Lopez J, Rodríguez-Ramos RFS, Alejandro M, Martin Campoy P (2016) A flexible and dynamic mission planning architecture for UAV swarm coordination. In: International conference on unmanned aircraft systems (ICUAS), pp 355–363
36. Sasikala E, Nandhakumar N (2015) An intelligent technique to detect jamming attack in wireless sensor networks (WSNs). Int J Fuzzy Syst 17:76–83
37. Sedjelmaci H, Senouci S, Ansari N (2017) Intrusion detection and ejection framework against lethal attacks in UAV-aided networks: a Bayesian game-theoretic methodology. IEEE Trans Intell Transp Syst 18(5):1143–1153
38. Shakhatreh H, Khreishah A, Chakareski J, Salameh H, Khalil I (2016) On the continuous coverage problem for a swarm of UAVs. In: 37th IEEE Sarnoff symposium, pp 1–6

39. Sherman T, Boskovich S (2019) UAV swarm mapping using a fully distributed control approach. In: AIAA Scitech 2019 forum, p 2287
40. Silva Arantes J, Silva Arantes M, Motta Toledo CF, Júnior OT, Williams BC (2017) Heuristic and genetic algorithm approaches for UAV path planning under critical situation. Int J Artif Intell Tools 26(01):1760008
41. Smyrnakis M, Kladis G, Aitken J, Veres S (2016) Distributed selection of flight formation in UAV missions. J Appl Math Bioinform 6(3):93–124
42. Srivastava D, Pakkar R, Langrehr A, Yamane C (2019) Adaptable UAV swarm autonomy and formation platform. In: IEEE aerospace conference. IEEE, New York, pp 1–6
43. Systems Tool Kit (STK). http://www.agi.com/products/stk/. Accessed 01 Nov 2019
44. Thakoor O, Garg J, Nagi R (2019) Multiagent UAV routing: a game theory analysis with tight price of anarchy bounds. IEEE Trans Autom Sci Eng 17:100–106
45. Vesterstrom J, Thomsen R (2004) A comparative study of differential evolution, particle swarm optimization, and evolutionary algorithms on numerical benchmark problems. In: Proceedings of the 2004 congress on evolutionary computation, vol 2, pp 1980–1987
46. Von Neumann J, Morgenstern O (2007) Theory of games and economic behavior. Princeton University Press, Princeton
47. Von Stackelberg H (2010) Market structure and equilibrium. Springer, Berlin
48. Wu H, Li H, Xiao R, Liu J (2018) Modeling and simulation of dynamic ant colony's labor division for task allocation of UAV swarm. Physica A 491:127–141
49. Yue L, Chen H (2019) Unmanned vehicle path planning using a novel ant colony algorithm. EURASIP J Wirel Commun Netw 2019(1):136
50. Zou J, Gundry S, Kusyk J, Uyar M, Sahin C (2013) 3D genetic algorithms for underwater sensor networks. Int Ad Hoc Ubiquitous Comput 13:10–22